Article:
Frandsen, KEH, Tovborg, M, Jørgensen, CI et al. (15 more authors) (2019) Insights into an unusual Auxiliary Activity 9 family member lacking the histidine brace motif of lytic polysaccharide monooxygenases. The Journal of Biological Chemistry, 294 (45). pp. 17117-17130. ISSN 0021-9258

https://doi.org/10.1074/jbc.ra119.009223

Insights into an unusual Auxiliary Activity 9 family member lacking the histidine brace motif of lytic polysaccharide monooxygenases

Kristian E. H. Frandsen[1,2], Morten Tovborg[3], Christian I. Jørgensen[3], Nikolaj Spodsberg[3], Marie-Noëlle Rosso[2], Glyn R. Hemsworth[4§,5], Elspeth F. Garman[6], Geoffrey W. Grime[7], Jens-Christian N. Poulsen[1], Tanveer S. Batth[8], Shingo Miyauchi[2], Anna Lipzen[9], Chris Daum[9], Igor V. Grigoriev[9,10], Katja S. Johansen[11], Bernard Henrissat[12,13,14] Jean-Guy Berrin[2], Leila Lo Leggio[1*].

Supporting information list:

Table S1

Supplementary Table 1. Peptides from *L.similis* induction secretomic data identified by ESI MS/MS

Start aa.	End aa.	Observed	Mr(expt)	Mr(calc)	ppm	Peptide score	Peptide sequence
22	49	1502.2344	3002.4543	3002.4543	-0.01	86	VPSSNAPVTDIESDDIICNTGFIQPVSK
50	70	1001.0167	2000.0189	2000.0228	-1.97	55	TVAAVPAGGTVIAHFHHTSAG
72	94	788.7539	2363.2397	2363.2373	1.04	27	VGPDPSDPLDPTNKGPVLAYLAK
76	94	666.0292	1995.0658	1995.0677	-0.93	47	PSDPLDPTNKGPVLAYLAK
79	94	566.3251	1695.9533	1695.9559	-1.54	45	PLDPTNKGPVLAYLAK
82	94	457.9369	1370.7889	1370.7922	-2.34	128	PTNKGPVLAYLAK
86	94	466.2835	930.5524	930.5538	-1.55	57	GPVLAYLAK
86	107	748.4152	2242.2238	2242.2209	1.28	27	GPVLAYLAKVPDATQSDVTGLK
92	107	548.3045	1641.8916	1641.8938	-1.32	28	LAKVPDATQSDVTGLK
95	107	665.8448	1329.6751	1329.6776	-1.93	79	VPDATQSDVTGLK
95	110	597.9813	1790.9219	1790.9203	0.9	136	VPDATQSDVTGLKWFK
108	121	590.3009	1767.8808	1767.8733	4.24	32	WFKIWQDGYTPATR
111	121	654.3212	1306.6279	1306.6306	-2.04	55	IWQDGYTPATR
152	182	1119.229	3354.665	3354.6554	2.86	97	VESISLLNAEQYPGAQFFLSCGQINITGGNK
169	182	754.8781	1507.7416	1507.7453	-2.48	65	FLSCGQINITGGNK

Amino acid (aa). The protein sequence coverage was 58%.

Table S2

Supplementary Table 2. Comparison of AA9 structures with *Ls*AA9B

Structure_chain	Number of residues	Number of aligned residues	percentage of residues aligned	Sequnce identity	rmsd (Å)
*Ls*AA9B_A	221	221	100	100	0.0
3EJA_A	208	154	74	42.9	1.79
4B5Q_A	217	192	88	35.9	1.45
5ACH_A	235	200	85	37.0	1.44
4D7U_A	227	214	94	45.8	1.04
4EIR_A	223	213	96	45.1	1.09
4QI8_A	214	154	72	42.2	1.80
5FOH_A	218	166	76	47.6	1.62
4EIS_A	225	198	88	39.9	1.46
3ZUD_A	228	199	87	33.7	1.50
2VTC_A	228	201	88	28.4	1.59

Superpose in CCP4 suite was used for calculation of RMSD C_α trace using Secondary-structure matching (SSM) (1,2)

Table S3

Supplementary Table 3. Quantitation of selected elements from PIXE analysis for *Ls*AA9B

	Element											
	16 S			**15 P**			**29 Cu**			**30 Zn**		
	Relative Conc*	No. of atoms	LOD†	Relative Conc*	No. of atoms	LOD†	Relative Conc*	No. of atoms	LOD†	Relative Conc*	No. of atoms	LOD†
*Ls*AA9B Point 1	12864.9	4‡	0.045	3600.7	1.16	0.027	68.7	0.011	0.0030	22.8	0.0035	0.0051
*Ls*AA9B Point 2	10125.2	4‡	0.047	2781.3	1.13	0.032	27.4	0.0055	0.0050	14.6	0.0028	0.0050
*Ls*AA9B Avg		4‡	0.046		1.15 (±0.03)	0.030		0.0082 (±0.0039)	0.0040		0.0032 (±0.0030)	0.0051

* Measured concentration (relative units, see ref (3))
† LOD = Limit of detection (atoms/protein molecule)
‡ Assumed values from protein sequence

Table S4

Supplementary Table 4. Glycosidic torsion angles					
		Reducing end		Non-reducing end	
Glycosidic torsion angles		Xyl1-Xyl2	Xyl2-Xyl3	Xyl3-Xyl4	Xyl4-Xyl5
*Ls*AA9B_Xyl4	Φ (°) Ψ(°) Φ+Ψ(°)	-116.7 (244.3) -53.8 (306.2) 550.5	-81.7 (278.4) 137.6 416	-117.9 (242.1) 158.1 400.2	-
*Ls*AA9A_Xyl5 (PDB 5NLO)	Φ (°) Ψ(°) Φ+Ψ(°)	-75.5 (284.5) -175.4 (184.6) 469.1 (subsite +1/+2)	-80.2 (279.8) 162.4 442.2 (subsite -1/+1)	-86.3 (273.7) 118.7 392.4 (subsite -2/-1)	-97.7 (262.3) 130.2 392.5 (subsite -3/-2)
Dihedral values as measured in COOT. Values in parenthesis are obtained by the addition of 360°. Φ+Ψ are the sum of positive Φ and Ψ values.					
Definitions	Φ	O5' – C1' – O4 – C4			
	Ψ	C1' – O4 – C4 – C3			
left-handed 3_1-fold helical screw					
Ideal values (inferred from ref (4))	Φ	290°			
	Ψ	130°			
	Φ+Ψ	420°			

Fig. S1

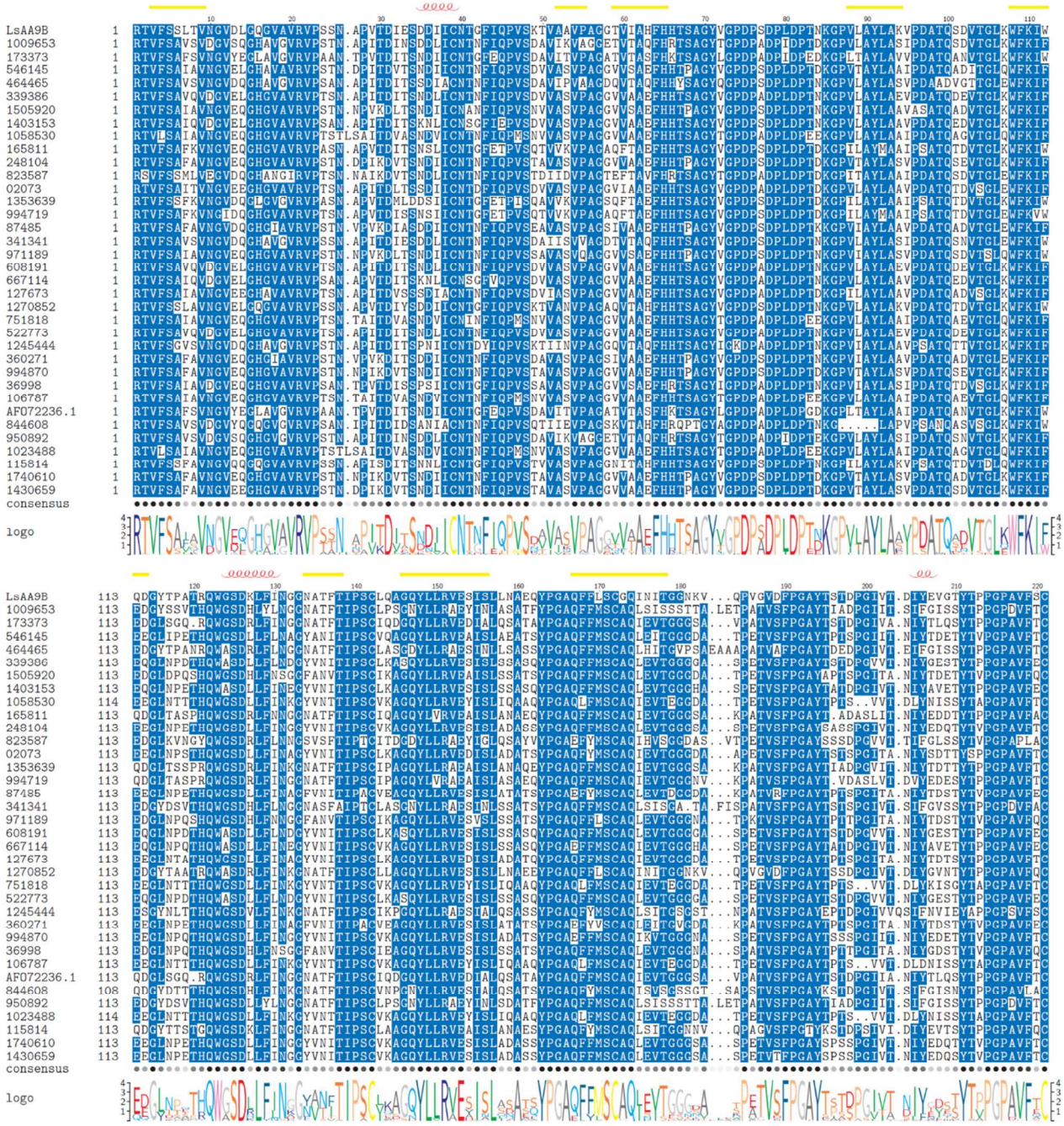

Supplementary Figure 1. Multiple sequence alignment of Arg-AA9s retrieved from CAZy. >50% sequence conservation is indicated with blue. JGI protein ID or GenBank ID (*Hi*AA9G; AFO72236.1) are given for each Arg-AA9. Secondary structure elements and numbering above the sequence are according to *Ls*AA9B. *Ls*AA9B R1, N84, L158, Q167 and F169 correspond to residues critical for LPMO function in canonical AA9 LPMOs (H1, H68, H142, Q151 and Y153 in *Tt*AA9E.) Logos below the sequences show the consensus between AA9s with N-terminal Arg. The most common substitutions of the critical residues compared to the canonical AA9s enzymes are H1 to R1, H68 to N84 (or D/E), H142 to L158 (or A/S/Q/I), Q151 to E (Q167 in *Ls*AA9B) and Y153 to F169 (numbering according to *Tt*AA9E substitutions to *Ls*AA9B). *Ls*AA9B N26, H66, T67, T83, N159, E161 and Y206 are equivalent to *Ls*AA9A N28, H66, N67, S77, E148, D150 and Y203, which are involved in *Ls*AA9A-oligosaccharide binding.

Fig. S2

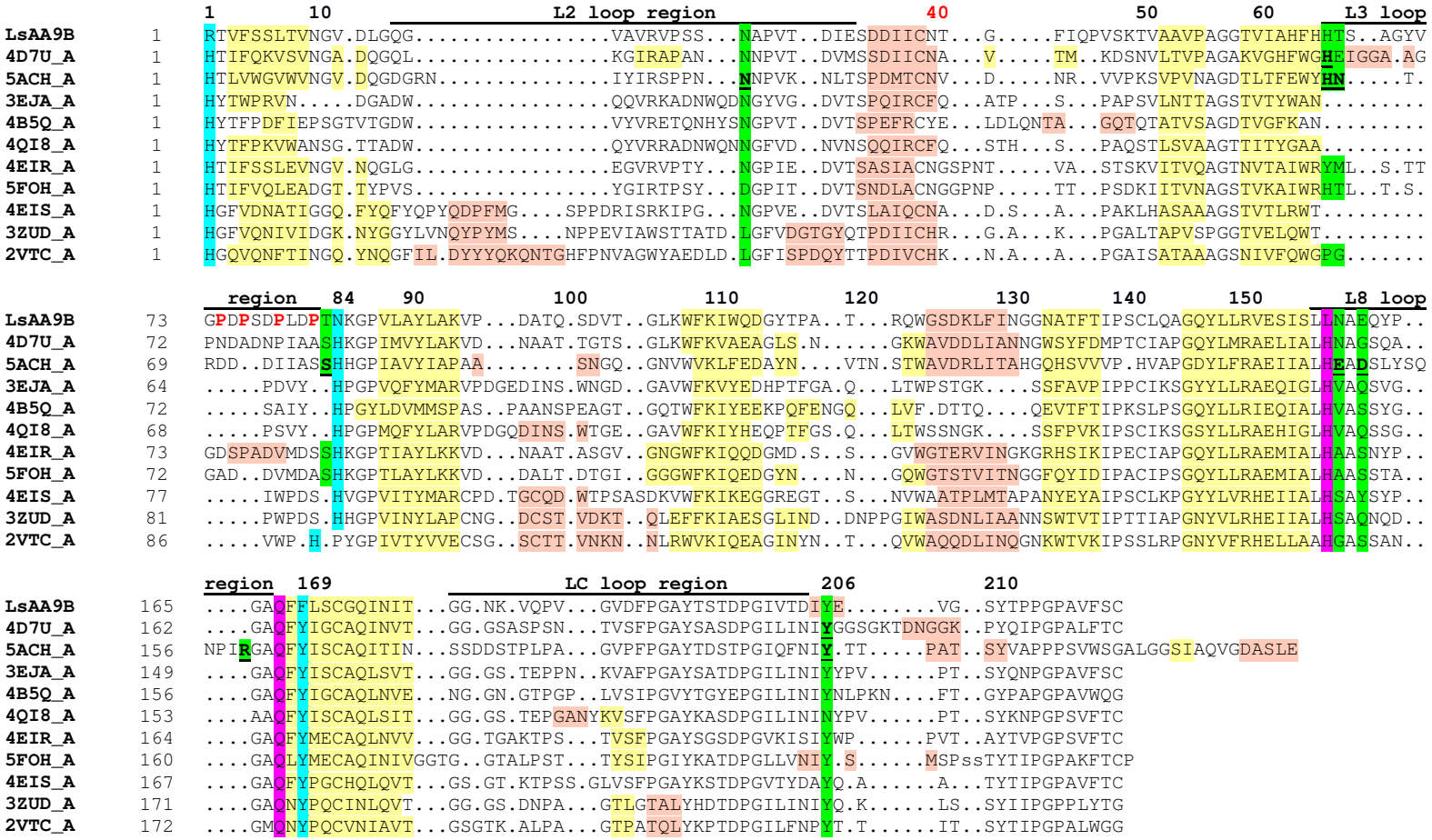

Supplementary Figure 2. Structure based sequence alignment of AA9 proteins

Secondary structure elements are coloured for all sequences in red and yellow for helices and β-strands, respectively. Positions of residues critical for AA9 LPMO activity are show in cyan and magenta for active site Cu coordinating residue positions and for positions in the secondary coordination sphere, respectively (these are R1, N84, F169, L158 and Q167 in *Ls*AA9B; H1, H78, H147, Q162 and Y164 in *Ls*AA9A (PDB code 5ACH) and H1, H68, H142, Q151 and Y153 in *Tt*AA9E (PDB code 3EJA)). Residues determined experimentally to be involved in cellooligosaccharides binding are in bold and underlined (N28, H66, N67, S77, E148, D150 and Y203 in *Ls*AA9A) and residues in equivalent positions are in green (N26, H66, T67, T83, N159, E161 and Y206 in *Ls*AA9B). Four conserved prolines found in AA9s with N-terminal Arg are in red and bold. The loop L2, loop L3, loop L8 and loop LC regions are indicated above the sequence. Numbering above the sequence are according to *Ls*AA9B.

Fig. S3

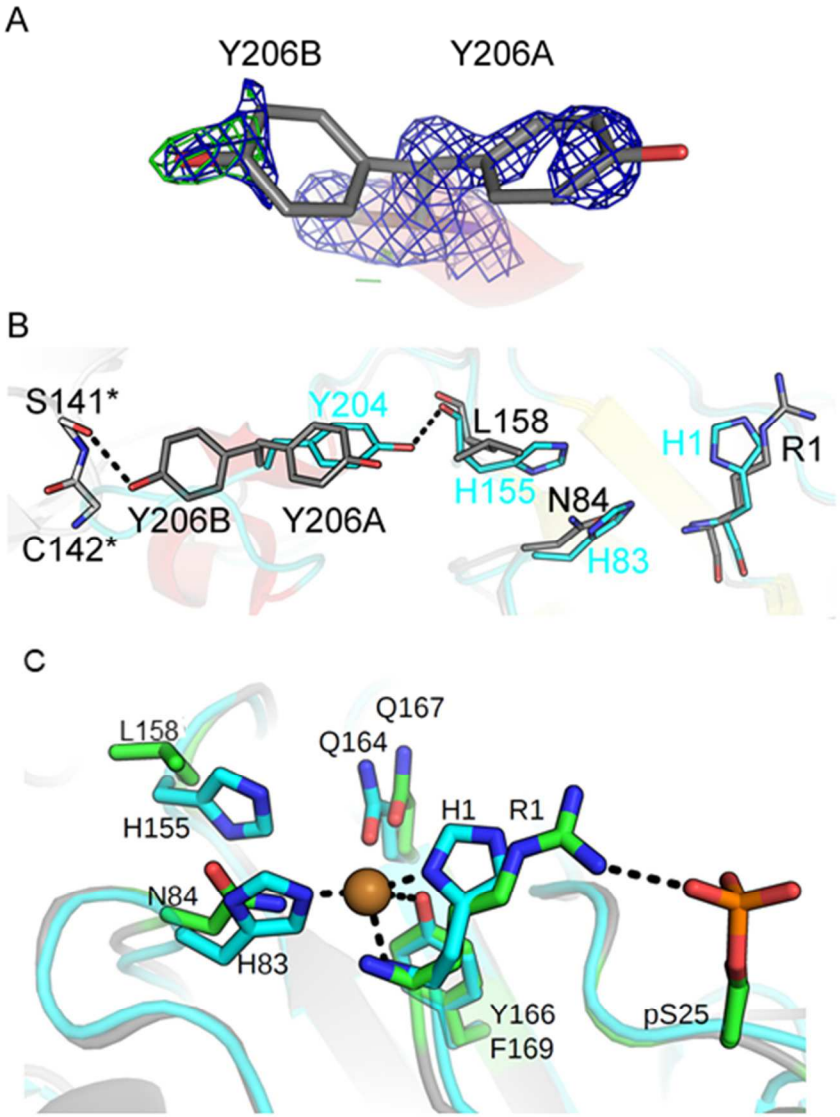

Supplementary Figure 3
(A) The disordered Y206 of *Ls*AA9B modelled in two conformations. The electron density maps 2Fo-Fc (blue) and Fo-Fc (green) contoured at 0.8σ and 2.5σ, respectively, are calculated from a structure before modelling an alternative conformation B. **(B)** Comparison of *Ls*AA9B (grey) and *Nc*AA9C (cyan). Symmetry-related molecules are shown in white and labelled with asterisk. **(C)** Superimposition of *Ls*AA9B (green) and *Nc*AA9C (PDB 4D7U, cyan) showing that the lack of metal binding is not due to occlusion by the phosphoserine.

Fig. S4

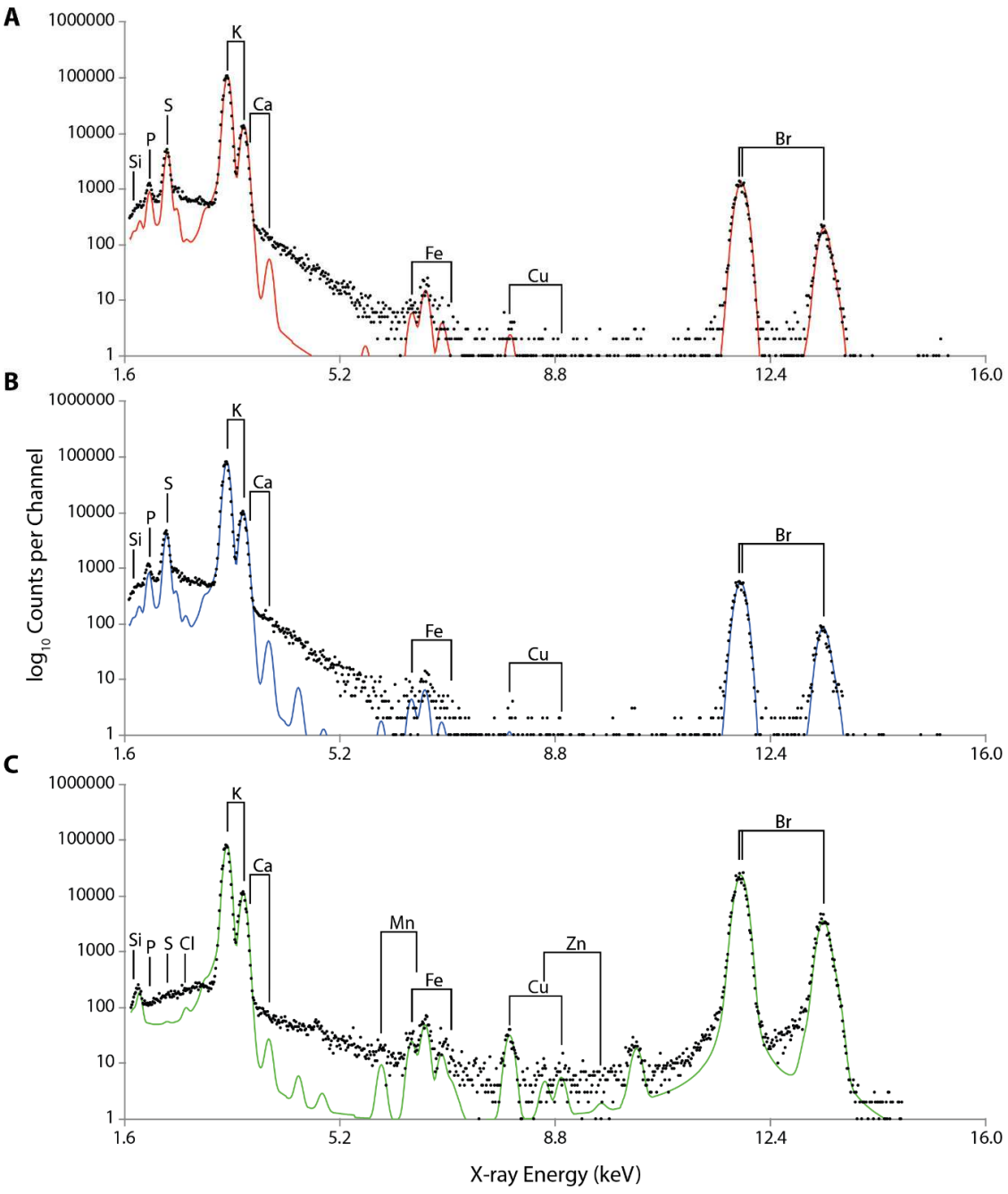

Supplementary Figure 4
Proton Induced X-ray Emission (PIXE) spectra (black points) and fit to the data (coloured lines) for **(A)** the first point spectrum measured on *Ls*AA9B, **(B)** the second point spectrum measured on LsAA9B and **(C)** a single point spectrum measured on the protein buffer alone as a control (n.b. lack of sulphur indicating sulphur peak in (A) and (B) are solely from the protein). The theoretical positions for X-ray emission maxima are indicated in all cases.

Supporting information references

1. Krissinel, E., and Henrick, K. (2004) Secondary-structure matching (SSM), a new tool for fast protein structure alignment in three dimensions. *Acta crystallographica. Section D, Biological crystallography* **60**, 2256-2268
2. Winn, M. D., Ballard, C. C., Cowtan, K. D., Dodson, E. J., Emsley, P., Evans, P. R., Keegan, R. M., Krissinel, E. B., Leslie, A. G., McCoy, A., McNicholas, S. J., Murshudov, G. N., Pannu, N. S., Potterton, E. A., Powell, H. R., Read, R. J., Vagin, A., and Wilson, K. S. (2011) Overview of the CCP4 suite and current developments. *Acta crystallographica. Section D, Biological crystallography* **67**, 235-242
3. Garman, E. F., and Grime, G. W. (2005) Elemental analysis of proteins by microPIXE. *Progress in biophysics and molecular biology* **89**, 173-205
4. Martinez-Abad, A., Berglund, J., Toriz, G., Gatenholm, P., Henriksson, G., Lindstrom, M., Wohlert, J., and Vilaplana, F. (2017) Regular Motifs in Xylan Modulate Molecular Flexibility and Interactions with Cellulose Surfaces. *Plant physiology* **175**, 1579-1592